

## Nonreciprocal photon blockade and directional amplification in a spinning resonator coupled to a two-level atom

Yu-Wei Jing,<sup>1</sup> Hai-Quan Shi,<sup>2</sup> and Xun-Wei Xu <sup>1,2,\*</sup>

<sup>1</sup>Key Laboratory of Low-Dimensional Quantum Structures and Quantum Control of Ministry of Education, Key Laboratory for Matter Microstructure and Function of Hunan Province, Department of Physics and Synergetic Innovation Center for Quantum Effects and Applications, Hunan Normal University, Changsha 410081, China

<sup>2</sup>Department of Applied Physics, East China Jiaotong University, Nanchang 330013, China



(Received 4 February 2021; accepted 30 August 2021; published 10 September 2021)

We propose a scheme to realize nonreciprocal photon blockade and directional amplification in a spinning resonator with clockwise and counterclockwise traveling modes coupled to a stationary two-level atom. By manipulating the rotational frequency of the resonator, the two-level atom can be resonant with one of the traveling modes and largely detuned from the other one. Nonreciprocal conventional photon blockade is induced by the difference of the detunings between the two-level atom and the optical modes traveling in different directions. Besides that, nonreciprocal unconventional photon blockade (UPB) based on the quantum interference can also be observed in the system. Based on the mechanism for nonreciprocal UPB, directional amplification of the blocked photons is predicted by driving the spinning resonator and stationary two-level atom simultaneously. Our proposal will be applicable to achieve highly efficient nonreciprocal single-photon devices for applications in chiral quantum information processing.

DOI: [10.1103/PhysRevA.104.033707](https://doi.org/10.1103/PhysRevA.104.033707)

### I. INTRODUCTION

Methods to create and manipulate quantum photon transport have drawn an immense amount of interest in the past decades, for their significance in quantum optics and quantum information processing [1]. One of the representative researches is the photon blockade phenomenon predicted by Imamoglu *et al.* in close analogy with the phenomenon of Coulomb blockade for quantum-well electrons [2]. Experimentally, photon blockade was first observed by Birnbaum *et al.* for the light transmitted by an optical cavity containing one trapped atom, in the regime of strong atom-cavity coupling [3]. Subsequently, photon blockade was reported on chip with different platforms, including an atom interacting with the evanescent fields of a microtoroidal resonator [4], a single quantum dot strongly coupled to a photonic-crystal cavity [5,6], and a qubit embedded in a transmission line [7,8]. The main ingredient to observe the conventional photon blockade (CPB) mentioned above is the strong photon-photon interaction, regardless of the physical origin of the interaction.

On the other hand, Liew and Savona reported a numerical study of a coupled cavity system and showed that strong photon antibunching can be obtained with a Kerr nonlinear coefficient much smaller than the cavity decay rate [9]. The origin of the strong antibunching was traced back to a sort of quantum interference effect, which was analytically unveiled by Bamba *et al.* [10] and the photon blockade based on this novel mechanism is referred to as unconventional photon blockade (UPB) [11–27]. UPB was demonstrated

experimentally by two independent teams, in two orthogonally polarized optical cavity modes [28] and two coupled superconducting resonators [29].

Recently, Huang *et al.* introduced nonreciprocal photon blockade to refer to the quantum effect that photon blockade happens when the system is driven in one direction but not for the other [30]. A spinning resonator with broken time-reversal symmetry provides an ideal platform for realization of nonreciprocal devices [31–33], and several proposals for nonreciprocal photon blockade were suggested based on this platform, such as a spinning Kerr resonator [30], a spinning optomechanical resonator [34], a spinning resonator with a second-order nonlinearity [35], a spinning resonator immersed in a degenerate optical parametric amplifier [36], and a spinning resonator resonantly coupled to a two-level atom [37]. Nonreciprocal photon blockade also has been proposed without using spinning resonators, such as in a quadratic optomechanical system based on directional nonlinear interaction [38] and in a three-mode system based on a combination of nonlinearity and synthetic magnetism [39]. Nonreciprocal nonclassical statistics were reported in a cavity quantum electrodynamical system with a few cesium atoms strongly coupled to a high-finesse Fabry-Pérot cavity [40].

Inspired by the fact that most of the experiments for photon blockade are performed based on the Jaynes-Cummings model [3–8], in this paper, we are going to discuss nonreciprocal photon blockade and directional amplification in a spinning resonator with the clockwise (CW) and counterclockwise (CCW) traveling modes coupled to a stationary two-level atom. More specifically, the resonator without spinning is largely detuned from the two-level atom, and when

\*davidxu0816@163.com

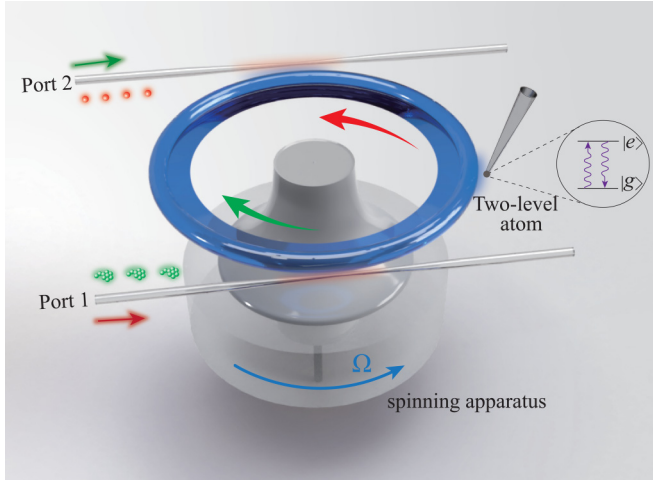


FIG. 1. Schematic diagram for a stationary two-level atom with a ground state  $|g\rangle$  and an excited state  $|e\rangle$  coupled to a spinning resonator with clockwise (CW) and counterclockwise (CCW) traveling modes,  $a_{cw}$  and  $a_{ccw}$ . By fixing the CCW rotation of the resonator with a frequency  $\Omega$ , we have effective frequency  $\omega_c + \Delta_F$  ( $\omega_c - \Delta_F$ ) for the CW (CCW) traveling mode, with the stationary resonance frequency  $\omega_c$  and rotation induced Sagnac-Fizeau shift  $\Delta_F$ .

the resonator is spinning in one direction, the detunings of the CW and CCW traveling modes from the two-level atom will be different: one becomes larger and one becomes smaller and even resonant with the two-level atom. Thus the photons transmitted in different directions will suffer different interactions. Differently from the previous proposal of nonreciprocal CPB in a resonator coupled to a two-level atom [37], we will show that not only nonreciprocal CPB but also nonreciprocal UPB based on the quantum interference can be observed in the system. Moreover, based on the mechanism for nonreciprocal UPB, directional amplification of the blockaded photons can emerge by driving the spinning resonator and stationary two-level atom simultaneously. Our proposal opens up a route to engineer quantum chiral devices, such as unidirectional single-photon quantum amplifiers, nonreciprocal single-photon routers, and single-photon isolators and circulators, based on the Jaynes-Cummings model.

The remainder of this paper is organized as follows. In Sec. II, we introduce the physical model of a spinning resonator coupled to a stationary two-level atom. In Sec. III, nonreciprocal CPB is proposed in the strong coupling regime. In Sec. IV, we show that nonreciprocal UPB can be observed in the weak coupling regime. In Sec. V, directional amplification of the blockaded photons are realized by driving the two-level atom coherently. Finally, the main results are summarized in Sec. VI.

## II. PHYSICAL MODEL

As shown in Fig. 1, the setup we consider here consists of a stationary two-level atom with a ground state  $|g\rangle$  and an excited state  $|e\rangle$ , coupled to a spinning resonator with clockwise (CW) and counterclockwise (CCW) traveling modes via the optical evanescent field. By fixing the CCW rotation of the resonator with a frequency  $\Omega$ , we have effective frequency

$\omega_c + \Delta_F$  ( $\omega_c - \Delta_F$ ) for the CW (CCW) traveling mode, with the stationary resonance frequency  $\omega_c$  and the rotation induced Sagnac-Fizeau shift

$$\Delta_F = \frac{nR\Omega\omega_c}{c} \left( 1 - \frac{1}{n^2} - \frac{\lambda}{n} \frac{dn}{d\lambda} \right), \quad (1)$$

where  $c$  and  $\lambda$  are the speed and wavelength of light in vacuum, and  $n$  and  $R$  are the refractive index and radius of the resonator, respectively. The dispersion term  $dn/d\lambda$  originates from the relativistic correction of the Sagnac effect, is relatively small, and can be ignored in typical materials [31,32]. As introduced above, the system can be described by a Hamiltonian ( $\hbar = 1$ )

$$H_{\text{sys}} = (\omega_c + \Delta_F) a_{cw}^\dagger a_{cw} + (\omega_c - \Delta_F) a_{ccw}^\dagger a_{ccw} + \omega_0 \sigma_+ \sigma_- + J(a_{cw} \sigma_+ + a_{ccw} \sigma_+ + \text{H.c.}), \quad (2)$$

where  $\sigma_+ \equiv |e\rangle\langle g|$  and  $\sigma_- \equiv |g\rangle\langle e|$  are the raising and lowering operators of the two-level atom with transition frequency  $\omega_0$ ;  $a_\eta$  and  $a_\eta^\dagger$  ( $\eta = cw, ccw$ ) are the annihilation and creation operators of the traveling mode; and  $J$  is the coupling strength between the two-level atom and traveling modes. In addition, we assume that the traveling mode  $a_\eta$  is coupled to the ports 1 and 2 of the tapered fibers via evanescent fields with strength  $\kappa/2$ .

To investigate the system's response behavior to a weak probe field, a weak laser with amplitude  $\varepsilon \ll \kappa$  and frequency  $\omega_p$  is input from one of the ports. Thus the total Hamiltonian is given by

$$H_{\text{tot}} = H_{\text{sys}} + H_{\text{probe}}, \quad (3)$$

with  $H_{\text{probe}}$  as

$$H_{\text{probe}} = \varepsilon e^{-i\omega_p t} a_\eta^\dagger + \text{H.c.}, \quad (4)$$

where  $\eta = ccw$  for the probe field input from port 1, or  $\eta = cw$  for the probe field input from port 2. In the rotating reference frame with the unitary operator  $U(t) = \exp[i\omega_p(a_{cw}^\dagger a_{cw} + a_{ccw}^\dagger a_{ccw} + \sigma_+ \sigma_-)t]$ ,  $H_{\text{tot}}$  becomes time independent,

$$H_{\text{tot}} = (-\Delta_c + \Delta_F) a_{cw}^\dagger a_{cw} + (-\Delta_c - \Delta_F) a_{ccw}^\dagger a_{ccw} - \Delta_0 \sigma_+ \sigma_- + J(a_{cw} \sigma_+ + a_{ccw} \sigma_+ + \text{H.c.}) + \varepsilon(a_\eta^\dagger + a_\eta), \quad (5)$$

with the detunings  $\Delta_0 \equiv \omega_p - \omega_0$ ,  $\delta \equiv \omega_c - \omega_0$ , and  $\Delta_c \equiv \omega_p - \omega_c = \Delta_0 - \delta$ .

According to the input-output relations [41], for probe photon transport from port 1 to port 2 with  $\eta = ccw$  in Eq. (5), we have  $a_{1,\text{in}} = \varepsilon/\sqrt{\kappa/2}$  and  $a_{2,\text{out}} = \sqrt{\kappa/2} a_{ccw}$ ; then the transmission coefficient for the weak probe field can be defined by

$$T_{21} \equiv \frac{\langle a_{2,\text{out}}^\dagger a_{2,\text{out}} \rangle}{\langle a_{1,\text{in}}^\dagger a_{1,\text{in}} \rangle} = \frac{\kappa^2}{4\varepsilon^2} \langle a_{ccw}^\dagger a_{ccw} \rangle, \quad (6)$$

and the statistic properties of the transmitted photons  $a_{2,\text{out}}$  can be described by the equal-time second-order correlation function in the steady state ( $t \rightarrow \infty$ )

$$g_{21}^{(2)}(0) \equiv \frac{\langle (a_{2,\text{out}}^\dagger)^2 (a_{2,\text{out}})^2 \rangle}{\langle a_{2,\text{out}}^\dagger a_{2,\text{out}} \rangle^2} = \frac{\langle (a_{ccw}^\dagger)^2 (a_{ccw})^2 \rangle}{\langle a_{ccw}^\dagger a_{ccw} \rangle^2}. \quad (7)$$

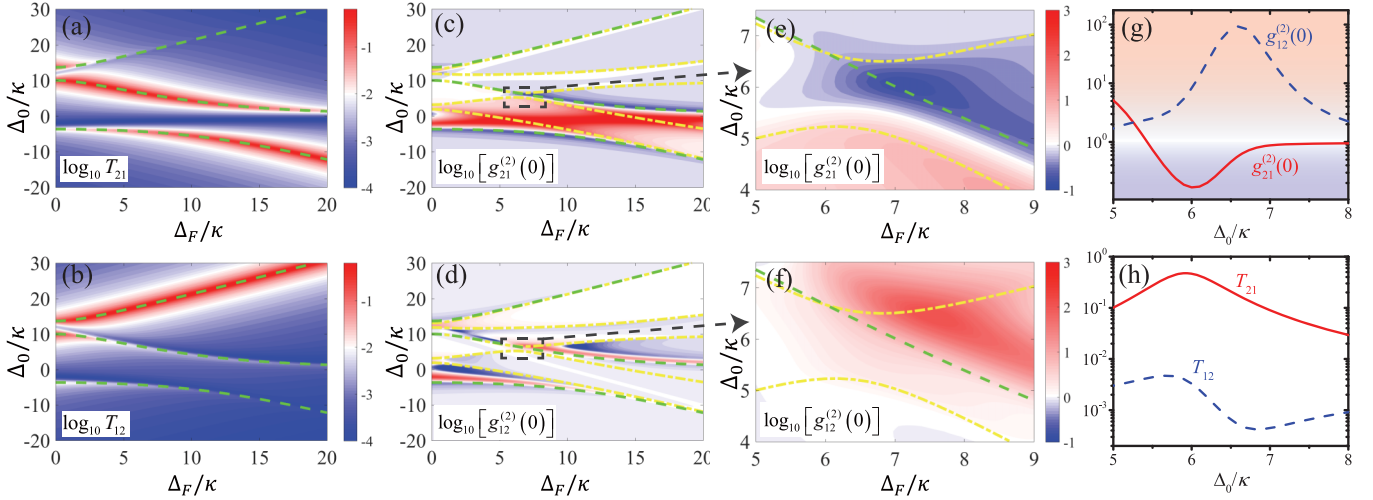


FIG. 2. (a) [(b)] The probe laser transmission spectra  $T_{21}$  from port 1 to port 2 [ $T_{12}$  from port 2 to port 1] as a function of the frequency shift  $\Delta_F$  and the detuning of the probe field  $\Delta_0$ . (c) [(d)] The second-order correlation function of the transited photons  $g_{21}^{(2)}(0)$  from port 1 to port 2 [ $g_{12}^{(2)}(0)$  from port 2 to port 1] as a function of the frequency shift  $\Delta_F$  and the detuning of the probe field  $\Delta_0$ . (e) and (f) are the magnifications of (c) and (d). (g)  $g_{21}^{(2)}(0)$  [ $g_{12}^{(2)}(0)$ ] and (h)  $T_{21}$  [ $T_{12}$ ] versus detuning of the probe field with  $\Delta_F = 7.16\kappa$ . The other parameters are taken as  $J = 5\kappa$ ,  $\delta = 10\kappa$ ,  $\varepsilon = 0.01\kappa$ , and  $\gamma = \kappa$ .

Similarly, for probe photon transport from port 2 to port 1 with  $\eta = cw$  in Eq. (5), we have  $a_{2,in} = \varepsilon/\sqrt{\kappa/2}$  and  $a_{1,out} = \sqrt{\kappa/2}a_{cw}$ ; then the transmission coefficient for the weak probe field can be defined by

$$T_{12} \equiv \frac{\langle a_{1,out}^\dagger a_{1,out} \rangle}{\langle a_{2,in}^\dagger a_{2,in} \rangle} = \frac{\kappa^2}{4\varepsilon^2} \langle a_{cw}^\dagger a_{cw} \rangle, \quad (8)$$

and the equal-time second-order correlation function in the steady state ( $t \rightarrow \infty$ ) is defined by

$$g_{12}^{(2)}(0) \equiv \frac{\langle (a_{1,out}^\dagger)^2 (a_{1,out})^2 \rangle}{\langle a_{1,out}^\dagger a_{1,out} \rangle^2} = \frac{\langle (a_{cw}^\dagger)^2 (a_{cw})^2 \rangle}{\langle a_{cw}^\dagger a_{cw} \rangle^2}. \quad (9)$$

In the following sections, based on the total Hamiltonian in Eq. (5), the transmission coefficients and second-order correlation functions will be obtained by numerically solving the master equation for density matrix  $\rho$  [42],

$$\frac{\partial \rho}{\partial t} = -i[H_{tot}, \rho] + \kappa L[a_{cw}]\rho + \kappa L[a_{ccw}]\rho + \gamma L[\sigma_-]\rho, \quad (10)$$

where  $L[o]\rho = o\rho o^\dagger - (o^\dagger o\rho + \rho o^\dagger o)/2$  denotes a Lindblad term for an operator  $o$ ;  $\gamma$  is the damping rate of the two-level atom.

### III. NONRECIPROCAL CPB

In Figs. 2(a) and 2(b), we show the transmission spectra  $T_{21}$  for probe field transport from port 1 to port 2, and  $T_{12}$  for probe field transport from port 2 to port 1 versus the frequency shift  $\Delta_F$  and the detuning  $\Delta_0$ . The three green dashed curves show the one-photon resonant conditions (see Appendix A for details), which agree well with the peaks in the transmission spectra; that is to say, the transmission spectra are mainly dependent on the one-photon resonant conditions under the weak driving condition  $\varepsilon = 0.01\kappa$ . The figures clearly show  $T_{21} \neq T_{12}$  when  $\Delta_F \neq 0$  for the probe field input from different transport directions exciting different traveling

modes. Specifically, the CCW traveling mode is excited for photon transport from port 1 to port 2 and the CW traveling mode is excited for photon transport from port 2 to port 1. In this section,  $|g, n_{ccw}, n_{cw}\rangle$  ( $|e, n_{ccw}, n_{cw}\rangle$ ) denotes the eigenstate of the two-level atom in the ground (excited) state and  $n_{ccw}$  ( $n_{cw}$ ) photons in the CCW (CW) traveling mode. In the strong coupling regime  $J = 5\kappa$ , there is an anticrossing between the energy levels  $|e, 0, 0\rangle$  and  $|g, 1, 0\rangle$  around the frequency shift  $\Delta_F = \delta$ , so that there are two peaks for photon transport from port 1 to port 2 under the one-photon resonant conditions. In contrast, there is one peak under the one-photon resonant condition around the frequency of  $(-\Delta_c - \Delta_F)$  for photon transport from port 2 to port 1, because the effect of the coupling between the energy levels  $|e, 0, 0\rangle$  and  $|g, 0, 1\rangle$  becomes weaker for the monotonic increase of detuning ( $\delta + \Delta_F$ ) with increasing frequency shift  $\Delta_F$ .

There are two different mechanisms for photon blockade: one is due to the strong anharmonicity, i.e., CPB; the other one is due to the destructive interference between different paths for two-photon excitation, i.e., UPB (we will discuss UPB in the next section). In Figs. 2(c) and 2(d), the second-order correlation functions  $g_{21}^{(2)}(0)$  and  $g_{12}^{(2)}(0)$  are plotted as functions of the frequency shift  $\Delta_F$  and the detuning of the probe field  $\Delta_0$ . The three green dashed curves show the one-photon resonant conditions and the five yellow dashed-dot curves show the two-photon resonant conditions (see Appendix A for details). In the strong coupling regime  $J = 5\kappa$ , the CPB appears when the probe field is resonant with the one-photon resonant conditions but is also off-resonant from the two-photon resonant conditions, as shown in Figs. 2(e) and 2(f). To compare the results for photon transport in different directions, we show  $g_{21}^{(2)}(0)$  and  $g_{12}^{(2)}(0)$  versus  $\Delta_0$  with  $\Delta_F = 7.16\kappa$  in the same figure, i.e., Fig. 2(g). We also show  $T_{21}$  and  $T_{12}$  versus  $\Delta_0$  with the same parameters in Fig. 2(h). As different traveling modes are excited for the probe field input from different directions, the system show both  $g_{21}^{(2)}(0) < 1 < g_{12}^{(2)}(0)$  and  $T_{21} \gg T_{12}$ , simultaneously. Physically, we have CPB with high

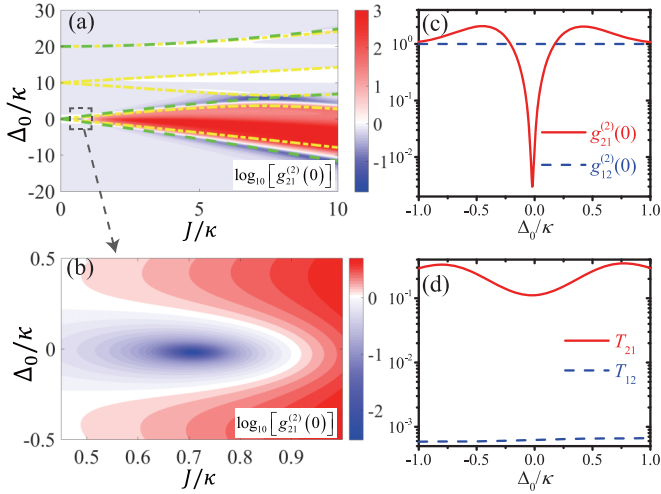


FIG. 3. (a) The second-order correlation function of the transited photons  $g_{21}^{(2)}(0)$  from port 1 to port 2 as a function of the coupling strength  $J$  and the detuning of the probe field  $\Delta_0$ . (b) is the magnification of (a). (c)  $g_{21}^{(2)}(0)$  [ $g_{12}^{(2)}(0)$ ] and (d)  $T_{21}$  [ $T_{12}$ ] versus detuning of the probe field  $\Delta_0$  with  $J = \kappa/\sqrt{2}$ . The other parameters are taken as  $\Delta_F = 10\kappa$ ,  $\delta = 10\kappa$ ,  $\varepsilon = 0.01\kappa$ , and  $\gamma = \kappa$ .

transitivity for photon transport from port 1 to port 2, and photon bunching with low transitivity for photon transport from port 2 to port 1.

#### IV. NONRECIPROCAL UPB

In Fig. 3(a), we show the second-order correlation functions  $g_{21}^{(2)}(0)$  versus the coupling strength  $J$  and the detuning  $\Delta_0$ . It is clear that the CPB [i.e., the dark blue regimes in Fig. 3(a)] appears in the strong coupling regime  $J > \kappa$  when the probe field is resonant with the one-photon resonant conditions (green dashed curves) but is also off resonant from the two-photon resonant conditions (yellow dashed-dot curves).

More interestingly, photon blockade also can be observed in the weak coupling regime (i.e., UPB) as shown in Fig. 3(b), where the strong photon antibunching appears around the optimal parameters  $J \approx 0.7\kappa$  and  $\Delta_0 = 0$  for photon transport from port 1 to port 2. But UPB does not appear for photon transport from port 2 to port 1, as shown in Fig. 3(c). In the meanwhile, we have nonreciprocal transmission coefficients with  $T_{21} \gg T_{12}$ , as shown in Fig. 3(d). So we have nonreciprocal UPB with high transmittance for photons transport from port 1 to port 2, and coherent photons with low transmittance for photon transport from port 2 to port 1.

To reveal the physical mechanism for nonreciprocal UPB, we need to rewrite the Hamiltonian with the parameter used in Fig. 3. As  $\Delta_F = \delta \gg \kappa$ , we have that  $-\Delta_c - \Delta_F = -\Delta_0$  and  $-\Delta_c + \Delta_F = -\Delta_0 + 2\Delta_F$ , i.e., the two-level atom is resonant with CCW traveling mode and largely detuned from the CW traveling mode. At the same time, the coupling strengths between the two-level atom and the traveling modes are weak, i.e.,  $J < \kappa$ , so the interaction terms between the two-level atom and the CW traveling mode are negligible. The effective Hamiltonian for photon transport from port 1 to port 2 can be

written as

$$H_{21} = -\Delta_0(\sigma_+\sigma_- + a_{\text{ccw}}^\dagger a_{\text{ccw}}) + J(a_{\text{ccw}}\sigma_+ + \text{H.c.}) + \varepsilon(a_{\text{ccw}}^\dagger + a_{\text{ccw}}), \quad (11)$$

and the effective Hamiltonian for photon transport from port 2 to port 1 is given by

$$H_{12} = (-\Delta_0 + 2\Delta_F)a_{\text{cw}}^\dagger a_{\text{cw}} + \varepsilon(a_{\text{cw}}^\dagger + a_{\text{cw}}). \quad (12)$$

$H_{12}$  describes a linear resonator driven by a weak coherent field, so the transmitted photons are coherent, i.e.,  $g_{12}^{(2)}(0) \approx 1$ , and  $T_{12} \ll 1$  around  $\Delta_0 = 0$  for large detuning  $(-\Delta_0 + 2\Delta_F) \gg \kappa$ . In contrast,  $H_{21}$  is the Hamiltonian of the system for a two-level atom resonant interacting with a single-mode resonator by the Jaynes-Cummings model [3–8]. The UPB is induced by the destructive quantum interference between the two paths for two-photon excitation: (i)  $|g, 1\rangle \rightarrow |g, 2\rangle$ ; (ii)  $|g, 1\rangle \rightarrow |e, 0\rangle \rightarrow |e, 1\rangle \rightarrow |g, 2\rangle$ . Here,  $|g, n_{\text{ccw}}\rangle$  ( $|e, n_{\text{ccw}}\rangle$ ) denotes the eigenstate of the two-level atom in the ground (excited) state and  $n_{\text{ccw}}$  photons in the CCW traveling mode. The conditions for the appearance of UPB can be understood in the following way. For  $\Delta_0 = 0$ , the amplitude for transition  $|g, 1\rangle \xrightarrow{\sqrt{2}\varepsilon} |g, 2\rangle$  is proportional to  $\sqrt{2}\varepsilon$  and the amplitude for transition  $|g, 1\rangle \xrightarrow{J} |e, 0\rangle \xrightarrow{\varepsilon} |e, 1\rangle \xrightarrow{\sqrt{2}J} |g, 2\rangle$  is proportional to  $4\sqrt{2}\varepsilon J^2/[\gamma(\gamma + \kappa)]$ , where the decay rates of the states  $|e, 0\rangle$  and  $|e, 1\rangle$ , i.e.,  $\gamma/2$  and  $(\gamma + \kappa)/2$ , are taken into consideration. The UPB as well as the destructive quantum interference are achieved when the coefficients of these two paths of photon excitation have the same amplitude but inverse phase, thus we obtain the optimal condition  $J_{\text{opt}} = \sqrt{\gamma(\gamma + \kappa)}/2$ . This is consistent well with the numerical results in Fig. 3(b) and the analytical result given in Appendix B.

#### V. DIRECTIONAL AMPLIFICATION OF BLOCKADED PHOTONS

Despite the nonreciprocity  $T_{21} \gg T_{12}$  as shown in Fig. 3(d), only ten percent of the photons are transported from port 1 to port 2, i.e.,  $T_{21} \approx 0.1$  for UPB. In order to enhance the intensity of the single-photon output from port 2, we assume that the two-level atom is driven by another coherent field with the same frequency  $\omega_p$ ; see Fig. 4(a). Then the total Hamiltonian can be rewritten as

$$H_{\text{tot}} = (-\Delta_c + \Delta_F)a_{\text{cw}}^\dagger a_{\text{cw}} + (-\Delta_c - \Delta_F)a_{\text{ccw}}^\dagger a_{\text{ccw}} - \Delta_0\sigma_+\sigma_- + J(a_{\text{cw}}\sigma_+ + a_{\text{ccw}}\sigma_+ + \text{H.c.}) + (\varepsilon a_\eta^\dagger + \varepsilon_d e^{-i\phi}\sigma_+ + \text{H.c.}), \quad (13)$$

where  $\varepsilon_d$  is the driving strength and  $\phi$  is the phase difference between the two coherent driving fields. The numerical results in Fig. 4 are calculated by substituting this total Hamiltonian into the master equation (10).

To obtain the optimal conditions for UPB analytically, we will consider the special case that the system is working under the resonant condition  $\Delta_0 = \Delta_c + \Delta_F$  and weak coupling condition  $J < \kappa \ll \Delta_F$ ; then the effective Hamiltonian for photon transport from port 1 to port 2 can be rewritten as

$$\tilde{H}_{21} = -\Delta_0(\sigma_+\sigma_- + a_{\text{ccw}}^\dagger a_{\text{ccw}}) + J(a_{\text{ccw}}\sigma_+ + \text{H.c.}) + (\varepsilon a_{\text{ccw}}^\dagger + \varepsilon_d e^{-i\phi}\sigma_+ + \text{H.c.}). \quad (14)$$

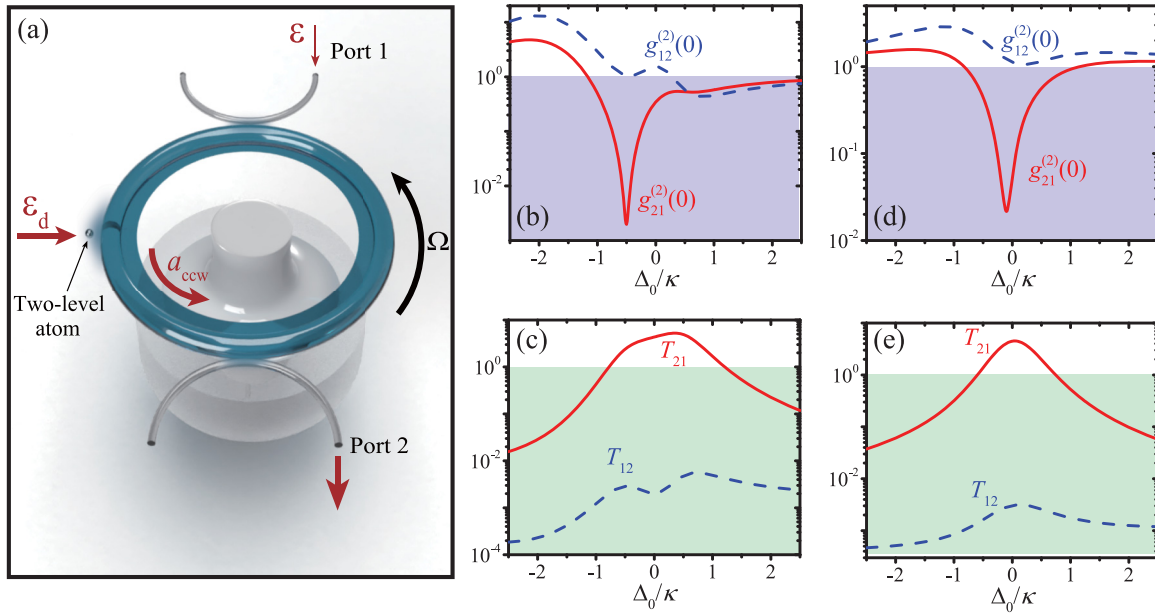


FIG. 4. (a) Schematic of the system working as a directional amplifier. (b) and (d)  $g_{21}^{(2)}(0)$  [ $g_{12}^{(2)}(0)$ ] versus detuning of the probe field  $\Delta_0$ ; (c) and (e)  $T_{21}$  [ $T_{12}$ ] versus detuning of the probe field  $\Delta_0$ . We set  $J = \kappa/2$  in (b) and (c),  $J = \kappa/10$  in (d) and (e). The other parameters are taken as  $\Delta_F = 10\kappa$ ,  $\delta = 10\kappa$ ,  $\epsilon = 0.01\kappa$ ,  $\epsilon_d = \epsilon\zeta_+ \exp(-i\phi_+)$ , and  $\gamma = \kappa$ .

Differently from the case with one driving field, the optimal condition to observe UPB with two driving fields is given by

$$\zeta_{\pm} e^{-i\phi_{\pm}} = -\frac{\Lambda_2}{J_{\text{opt}}} \pm \sqrt{\frac{\Lambda_1}{J_{\text{opt}}} \frac{\Lambda_2}{J_{\text{opt}}} - 1}. \quad (15)$$

with  $\zeta \equiv \epsilon_d/\epsilon$ ,  $\Lambda_1 = \Delta_{0,\text{opt}} + i\kappa/2$ , and  $\Lambda_2 = 2\Delta_{0,\text{opt}} + i(\gamma + \kappa)/2$ .  $\Delta_{0,\text{opt}}$  and  $J_{\text{opt}}$  are the parameters we can choose for UPB. The details of the derivation for Eq. (15) are given in Appendix B.

In Figs. 4(b) and 4(c), we show the second-order correlation functions  $g_{21}^{(2)}(0)$  and  $g_{12}^{(2)}(0)$ , and the transmission spectra  $T_{21}$  and  $T_{12}$ , versus the detuning  $\Delta_0$ , with the optimal parameters  $J = J_{\text{opt}} = 0.5\kappa$  and  $\Delta_{0,\text{opt}} = -J$ . Clearly, the system exhibits nonreciprocal UPB, i.e.,  $g_{21}^{(2)}(0) < 1 < g_{12}^{(2)}(0)$  and  $T_{21} \gg T_{12}$  in the weak coupling regime  $J < \kappa$ . Differently from the Figs. 2 and 3, we have  $T_{21} > 1 \gg T_{12}$  around the optimal detuning  $\Delta_{0,\text{opt}} = -J$ , i.e., the photon transport from port 1 to port 2 is amplified, whereas the transmission in the opposite direction is still very low. Physically, the amplification of the probe field results from the energy conversion due to the existence of the coherent driving field applied to the two-level atom. The transmission coefficient  $T_{21}$  can be even higher, as shown in Figs. 4(d) and 4(e), but we need much stronger external driving strength  $\epsilon_d$ . Finally, we would like to emphasize that, unlike previous works on directional amplification [43–47], the amplified output field exhibits strong antibunching effects even though all the driving fields are coherent.

## VI. DISCUSSIONS AND CONCLUSIONS

Let us now discuss the experimental requirements for our proposal. As strong coupling between one atom and a monolithic microresonator has been observed [4,48], the

key parameter for experimental demonstration is the angular velocity of the spinning resonator. With the experimentally feasible parameter values for microtoroidal resonators [48–54],  $\lambda = 1550$  nm,  $Q \sim 10^8$ – $10^{12}$ ,  $R = 22$   $\mu\text{m}$ ,  $n = 1.44$ ,  $\gamma = \kappa \simeq 2\pi \times 1$  MHz, we can estimate that the required Sagnac-Fizeau shift  $\Delta_F = 10\kappa \simeq 2\pi \times 10$  MHz is obtained with angular velocity  $\Omega \simeq 2\pi \times 150$  kHz. We have also confirmed that by using the experimental parameters of the spinning resonator (radius  $R = 4.75$  mm and angular velocity  $\Omega \simeq 2\pi \times 3$  kHz) as adopted in the experiment [32], all the nonreciprocal features we predicted in this manuscript can be achieved. Also, we note that even for smaller angular velocity  $\Omega \simeq 6.6$  kHz quantum nonreciprocal features still can be achieved as confirmed in various previous works based on spinning devices (see Refs. [30,34,55]).

In summary, we have demonstrated that nonreciprocal photon blockade and directional amplification can be observed in a spinning resonator for the supported CW and CCW traveling modes coupled to a stationary two-level atom with different detunings. We explicitly showed that both nonreciprocal CPB and UPB can be observed in the system. The nonreciprocal CPB appears in the strong coupling regime when the probe field is resonant with the one-photon resonant conditions but is also off-resonant from the two-photon resonant conditions. The nonreciprocal UPB is induced by the destructive quantum interference between the two paths for two-photon excitation in one traveling mode but not in the other traveling mode. Moreover, a directional amplifier of the blockaded photons is proposed by driving the optical mode and the two-level atom simultaneously. This physical model can also be extended to the case that the spinning resonator is coupled to other nonlinear systems, such as a resonator with  $\chi^{(2)}$  nonlinearity [56,57] or  $\chi^{(3)}$  nonlinearity [58–60], optomechanical interaction [61], degenerate optical parametric amplifiers [62], or graphene plasmonics [63,64]. Our proposal will be applicable to achieve

highly efficient nonreciprocal single-photon devices, such as unidirectional single-photon quantum amplifiers, nonreciprocal single-photon routers, and single-photon isolators and circulators, for applications in chiral and topological quantum technologies.

### ACKNOWLEDGMENTS

This work is supported by the National Natural Science Foundation of China under Grant No. 12064010, the Natural Science Foundation of Jiangxi Province of China under Grant No. 20192ACB21002, the Natural Science Foundation of Hunan Province of China under Grant No. 2021JJ20036, and the science and technology innovation Program of Hunan Province of China under Grant No. 2020RC4047.

### APPENDIX A: THE DERIVATION OF THE ONE- AND TWO-PHOTON RESONANT CONDITIONS

To understand the optimal conditions for CPB in the system, we will show how to get one-photon and two-photon resonant conditions in this Appendix. The eigenstate of the

$$H_{\text{sys}}^{(2)} = \begin{pmatrix} (-\Delta_c - \Delta_F - \Delta_0) & 0 & \sqrt{2}J & J & 0 \\ 0 & (-\Delta_c + \Delta_F - \Delta_0) & 0 & J & \sqrt{2}J \\ \sqrt{2}J & 0 & 2(-\Delta_c - \Delta_F) & 0 & 0 \\ J & J & 0 & 2(-\Delta_c) & 0 \\ 0 & \sqrt{2}J & 0 & 0 & 2(-\Delta_c + \Delta_F) \end{pmatrix}. \quad (\text{A2})$$

The eigenvalues  $E^{(2)}$  of the Hamiltonian  $H_{\text{sys}}^{(2)}$  are obtained by  $|H_{\text{sys}}^{(2)} - E^{(2)}I| = 0$ . The two-photon resonant conditions are that the frequency of the probe field  $\omega_p$  equals one-half of the eigenvalues  $E^{(2)}$ , i.e.,  $\omega_p = E^{(2)}/2$ .

### APPENDIX B: THE DERIVATION OF THE OPTIMAL CONDITIONS FOR UPB

We assume that both the CCW traveling mode and the two-level atom are driven by coherent fields with the same frequency  $\omega_p$ ; see Fig. 4(a). We will consider the special case that the system is working under the resonant condition  $\Delta_0 = \Delta_c + \Delta_F$  and weak coupling condition  $J < \kappa \ll \Delta_F$ ; then the effective Hamiltonian for photon transport from port 1 to port 2 can be rewritten as Eq. (14) in the main text.

In order to find the optimal condition for photon blockade of the photons transmitted from port 1 to port 2 through the CCW traveling mode, we use the ansatz

$$|\psi\rangle_{21} = C_{g,0}|g, 0\rangle + C_{e,0}|e, 0\rangle + C_{g,1}|g, 1\rangle + C_{e,1}|e, 1\rangle + C_{g,2}|g, 2\rangle, \quad (\text{B1})$$

where  $|g, n_{\text{ccw}}\rangle$  ( $|e, n_{\text{ccw}}\rangle$ ) denotes the eigenstate of the two-level atom in the ground (excited) state and  $n_{\text{ccw}}$  photons in the CCW traveling mode, with the corresponding occupying probability  $|C_{e, n_{\text{ccw}}}|^2$  ( $|C_{g, n_{\text{ccw}}}|^2$ ). Substitute the wave function  $|\psi\rangle_{21}$  and Hamiltonian  $\tilde{H}_{21}$  into the Schrodinger equation

two-level atom in the ground (excited) state and  $n_{\text{ccw}}$  ( $n_{\text{cw}}$ ) photons in the CCW (CW) traveling mode can be represented as  $|g, n_{\text{ccw}}, n_{\text{cw}}\rangle$  ( $|e, n_{\text{ccw}}, n_{\text{cw}}\rangle$ ). The weighted excitation number operator  $N = \sigma_+ \sigma_- + a_{\text{ccw}}^\dagger a_{\text{ccw}} + a_{\text{cw}}^\dagger a_{\text{cw}}$  is a conserved quantity for the commutative relation  $[N, H_{\text{sys}}] = 0$ . Thus the subspaces corresponding to different weighted excitation number  $N$  are separated from each other and we can obtain the one-photon and two-photon resonant conditions in different subspaces independently.

In the one-excitation subspace with bases  $\{|e, 0, 0\rangle, |g, 1, 0\rangle, |g, 0, 1\rangle\}$ , the Hamiltonian is

$$H_{\text{sys}}^{(1)} = \begin{pmatrix} -\Delta_0 & J & J \\ J & (-\Delta_c - \Delta_F) & 0 \\ J & 0 & (-\Delta_c + \Delta_F) \end{pmatrix}. \quad (\text{A1})$$

The eigenvalues  $E^{(1)}$  of the Hamiltonian  $H_{\text{sys}}^{(1)}$  are obtained by  $|H_{\text{sys}}^{(1)} - E^{(1)}I| = 0$ , where  $I$  is the identity matrix. The one-photon resonant conditions are that the frequency of the probe field  $\omega_p$  equals the eigenvalues  $E^{(1)}$ , i.e.,  $\omega_p = E^{(1)}$ .

In the two-excitation subspace with bases  $\{|e, 1, 0\rangle, |e, 0, 1\rangle, |g, 2, 0\rangle, |g, 1, 1\rangle, |g, 0, 2\rangle\}$ , the Hamiltonian is

$i\partial_t |\psi\rangle_{21} = \tilde{H}_{21} |\psi\rangle_{21}$ ; then we have

$$i\partial_t C_{e,0} = \left(-\Delta_0 - i\frac{\gamma}{2}\right)C_{e,0} + JC_{g,1} + \varepsilon C_{e,1} + \varepsilon_d e^{-i\phi} C_{g,0}, \quad (\text{B2})$$

$$i\partial_t C_{g,1} = \left(-\Delta_0 - i\frac{\kappa}{2}\right)C_{g,1} + JC_{e,0} + \varepsilon C_{g,0} + \sqrt{2}\varepsilon C_{g,2} + \varepsilon_d e^{i\phi} C_{e,1}, \quad (\text{B3})$$

$$i\partial_t C_{e,1} = \left(-2\Delta_0 - i\frac{\gamma + \kappa}{2}\right)C_{e,1} + \sqrt{2}JC_{g,2} + \varepsilon C_{e,0} + \varepsilon_d e^{-i\phi} C_{g,1}, \quad (\text{B4})$$

$$i\partial_t C_{g,2} = (-2\Delta_0 - i\kappa)C_{g,2} + \sqrt{2}JC_{e,1} + \sqrt{2}\varepsilon C_{g,1}. \quad (\text{B5})$$

As  $\{\varepsilon, \varepsilon_d\} \ll \{\kappa, \gamma\}$ , we have  $|C_{g,0}| \gg \{|C_{e,0}\rangle, |C_{g,1}\rangle\} \gg \{|C_{e,1}\rangle, |C_{g,2}\rangle\}$ . In the steady state, i.e.,  $i\partial_t C_{e/g, n_{\text{ccw}}} = 0$ , we have

$$0 = \left(-\Delta_0 - i\frac{\gamma}{2}\right)C_{e,0} + JC_{g,1} + \varepsilon_d e^{-i\phi} C_{g,0}, \quad (\text{B6})$$

$$0 = \left(-\Delta_0 - i\frac{\kappa}{2}\right)C_{g,1} + JC_{e,0} + \varepsilon C_{g,0}, \quad (\text{B7})$$

$$0 = \left(-2\Delta_0 - i\frac{\gamma + \kappa}{2}\right)C_{e,1} + \sqrt{2}JC_{g,2} + \varepsilon C_{e,0} + \varepsilon_d e^{-i\phi} C_{g,1}, \quad (\text{B8})$$

$$0 = (-2\Delta_0 - i\kappa)C_{g,2} + \sqrt{2}JC_{e,1} + \sqrt{2}\varepsilon C_{g,1}. \quad (\text{B9})$$

From Eqs. (B6) and (B7), we have

$$C_{e,0} = \frac{\varepsilon J + \varepsilon_d (\Delta_0 + i\frac{\kappa}{2}) e^{-i\phi}}{(\Delta_0 + i\frac{\gamma}{2})(\Delta_0 + i\frac{\kappa}{2}) - J^2} C_{g,0}, \quad (\text{B10})$$

$$C_{g,1} = \frac{J\varepsilon_d e^{-i\phi} + \varepsilon (\Delta_0 + i\frac{\gamma}{2})}{(\Delta_0 + i\frac{\gamma}{2})(\Delta_0 + i\frac{\kappa}{2}) - J^2} C_{g,0}. \quad (\text{B11})$$

To derive the optimal condition for photon blockade with  $C_{g,2} = 0$ , by substituting Eqs. (B10) and (B11) into Eqs. (B8) and (B9), we have

$$0 = \left(-2\Delta_0 - i\frac{\gamma + \kappa}{2}\right) C_{e,1} + \frac{\varepsilon^2 J + \varepsilon \varepsilon_d (2\Delta_0 + i\frac{\gamma + \kappa}{2}) e^{-i\phi} + J\varepsilon_d^2 e^{-i2\phi}}{(\Delta_0 + i\frac{\gamma}{2})(\Delta_0 + i\frac{\kappa}{2}) - J^2} C_{g,0}, \quad (\text{B12})$$

$$0 = \sqrt{2} J C_{e,1} + \sqrt{2} \varepsilon \frac{J\varepsilon_d e^{-i\phi} + \varepsilon (\Delta_0 + i\frac{\gamma}{2})}{(\Delta_0 + i\frac{\gamma}{2})(\Delta_0 + i\frac{\kappa}{2}) - J^2} C_{g,0}. \quad (\text{B13})$$

The condition for  $C_{e,1}$  and  $C_{g,0}$  to have nontrivial solutions is that the determinant of the coefficient matrices equals zero, and then we get the equation for optimal phonon antibunching

as

$$\begin{aligned} & (\zeta e^{-i\phi})^2 + \frac{2}{J_{\text{opt}}} \left(2\Delta_{0,\text{opt}} + i\frac{\gamma + \kappa}{2}\right) \zeta e^{-i\phi} + \frac{1}{J_{\text{opt}}^2} \left(\Delta_{0,\text{opt}} + i\frac{\gamma}{2}\right) \\ & \times \left(2\Delta_{0,\text{opt}} + i\frac{\gamma + \kappa}{2}\right) + 1 = 0, \end{aligned} \quad (\text{B14})$$

where  $\zeta \equiv \varepsilon_d/\varepsilon$ . If the driving field is not applied to the two-level atom, i.e.,  $\varepsilon_d = 0$  and  $\zeta = 0$ , the optimal conditions are written as

$$\Delta_{0,\text{opt}} = 0, \quad (\text{B15})$$

$$J_{\text{opt}} = \frac{1}{2} \sqrt{\gamma(\gamma + \kappa)}. \quad (\text{B16})$$

If  $\varepsilon_d \neq 0$  and  $\zeta \neq 0$ , then the two solutions of Eq. (B14) are given by

$$\begin{aligned} \zeta_{\pm} e^{-i\phi_{\pm}} = & - \left( \frac{2\Delta_{0,\text{opt}}}{J_{\text{opt}}} + i\frac{\gamma + \kappa}{2J_{\text{opt}}} \right) \\ & \pm \sqrt{\left( \frac{\Delta_{0,\text{opt}}}{J_{\text{opt}}} + i\frac{\kappa}{2J_{\text{opt}}} \right) \left( \frac{2\Delta_{0,\text{opt}}}{J_{\text{opt}}} + i\frac{\gamma + \kappa}{2J_{\text{opt}}} \right) - 1}. \end{aligned} \quad (\text{B17})$$

- 
- [1] I. Carusotto and C. Ciuti, Quantum fluids of light, *Rev. Mod. Phys.* **85**, 299 (2013).
- [2] A. Imamoglu, H. Schmidt, G. Woods, and M. Deutsch, Strongly Interacting Photons in a Nonlinear Cavity, *Phys. Rev. Lett.* **79**, 1467 (1997).
- [3] K. M. Birnbaum, A. Boca, R. Miller, A. D. Boozer, T. E. Northup, and H. J. Kimble, Photon blockade in an optical cavity with one trapped atom, *Nature (London)* **436**, 87 (2005).
- [4] B. Dayan, A. S. Parkins, T. Aoki, E. P. Ostby, K. J. Vahala, and H. J. Kimble, A photon turnstile dynamically regulated by one atom, *Science* **319**, 1062 (2008).
- [5] A. Faraon, I. Fushman, D. Englund, N. Stoltz, P. Petroff, and J. Vučković, Coherent generation of nonclassical light on a chip via photon-induced tunneling and blockade, *Nat. Phys.* **4**, 859 (2008).
- [6] A. Reinhard, T. Volz, M. Winger, A. Badolato, K. J. Hennessy, E. L. Hu, and A. Imamoglu, Strongly correlated photons on a chip, *Nat. Photonics* **6**, 93 (2011).
- [7] C. Lang, D. Bozyigit, C. Eichler, L. Steffen, J. M. Fink, A. A. Abdumalikov, M. Baur, S. Filipp, M. P. da Silva, A. Blais, and A. Wallraff, Observation of Resonant Photon Blockade at Microwave Frequencies Using Correlation Function Measurements, *Phys. Rev. Lett.* **106**, 243601 (2011).
- [8] A. J. Hoffman, S. J. Srinivasan, S. Schmidt, L. Spietz, J. Aumentado, H. E. Türeci, and A. A. Houck, Dispersive Photon Blockade in a Superconducting Circuit, *Phys. Rev. Lett.* **107**, 053602 (2011).
- [9] T. C. H. Liew and V. Savona, Single Photons from Coupled Quantum Modes, *Phys. Rev. Lett.* **104**, 183601 (2010).
- [10] M. Bamba, A. Imamoglu, I. Carusotto, and C. Ciuti, Origin of strong photon antibunching in weakly nonlinear photonic molecules, *Phys. Rev. A* **83**, 021802(R) (2011).
- [11] A. Majumdar, M. Bajcsy, A. Rundquist, and J. Vučković, Loss-Enabled Sub-Poissonian Light Generation in a Bimodal Nanocavity, *Phys. Rev. Lett.* **108**, 183601 (2012).
- [12] X.-W. Xu and Y.-J. Li, Antibunching photons in a cavity coupled to an optomechanical system, *J. Phys. B: At., Mol. Opt. Phys.* **46**, 035502 (2013).
- [13] H. Flayac and V. Savona, Input-output theory of the unconventional photon blockade, *Phys. Rev. A* **88**, 033836 (2013).
- [14] D. Gerace and V. Savona, Unconventional photon blockade in doubly resonant microcavities with second-order nonlinearity, *Phys. Rev. A* **89**, 031803(R) (2014).
- [15] X.-W. Xu and Y. Li, Strong photon antibunching of symmetric and antisymmetric modes in weakly nonlinear photonic molecules, *Phys. Rev. A* **90**, 033809 (2014).
- [16] X.-W. Xu and Y. Li, Tunable photon statistics in weakly nonlinear photonic molecules, *Phys. Rev. A* **90**, 043822 (2014).
- [17] O. Kyriienko, I. A. Shelykh, and T. C. H. Liew, Tunable single-photon emission from dipolaritons, *Phys. Rev. A* **90**, 033807 (2014).
- [18] O. Kyriienko and T. C. H. Liew, Triggered single-photon emitters based on stimulated parametric scattering in weakly nonlinear systems, *Phys. Rev. A* **90**, 063805 (2014).
- [19] E. Zubizarreta Casalengua, J. C. López Carreño, F. P. Laussy, and E. D. Valle, Conventional and unconventional photon statistics, *Laser Photonics Rev.* **14**, 1900279 (2020).
- [20] M.-A. Lecomte, N. Didier, and A. A. Clerk, Antibunching and unconventional photon blockade with Gaussian squeezed states, *Phys. Rev. A* **90**, 063824 (2014).
- [21] H. Z. Shen, Y. H. Zhou, and X. X. Yi, Tunable photon blockade in coupled semiconductor cavities, *Phys. Rev. A* **91**, 063808 (2015).
- [22] Y. H. Zhou, H. Z. Shen, and X. X. Yi, Unconventional photon blockade with second-order nonlinearity, *Phys. Rev. A* **92**, 023838 (2015).

- [23] J. Tang, W. Geng, and X. Xu, Quantum interference induced photon blockade in a coupled single quantum dot-cavity system, *Sci. Rep.* **5**, 9252 (2015).
- [24] H. Flayac and V. Savona, Unconventional photon blockade, *Phys. Rev. A* **96**, 053810 (2017).
- [25] J.-B. You, X. Xiong, P. Bai, Z.-K. Zhou, R.-M. Ma, W.-L. Yang, Y.-K. Lu, Y.-F. Xiao, C. E. Png, F. J. Garcia-Vidal, C.-W. Qiu, and L. Wu, Reconfigurable photon sources based on quantum plexcitonic systems, *Nano Lett.* **20**, 4645 (2020).
- [26] F. Zou, D.-G. Lai, and J.-Q. Liao, Enhancement of photon blockade effect via quantum interference, *Opt. Express* **28**, 16175 (2020).
- [27] F. Zou, X.-Y. Zhang, X.-W. Xu, J.-F. Huang, and J.-Q. Liao, Multiphoton blockade in the two-photon Jaynes-Cummings model, *Phys. Rev. A* **102**, 053710 (2020).
- [28] H. J. Snijders, J. A. Frey, J. Norman, H. Flayac, V. Savona, A. C. Gossard, J. E. Bowers, M. P. Van Exter, D. Bouwmeester, and W. Löffler, Observation of the Unconventional Photon Blockade, *Phys. Rev. Lett.* **121**, 043601 (2018).
- [29] C. Vaneph, A. Morvan, G. Aiello, M. Féchant, M. Aprili, J. Gabelli, and J. Estève, Observation of the Unconventional Photon Blockade in the Microwave Domain, *Phys. Rev. Lett.* **121**, 043602 (2018).
- [30] R. Huang, A. Miranowicz, J.-Q. Liao, F. Nori, and H. Jing, Nonreciprocal Photon Blockade, *Phys. Rev. Lett.* **121**, 153601 (2018).
- [31] G. B. Malykin, The Sagnac effect: Correct and incorrect explanations, *Phys. Usp.* **43**, 1229 (2000).
- [32] S. Maayani, R. Dahan, Y. Kligerman, E. Moses, A. U. Hassan, H. Jing, F. Nori, D. N. Christodoulides, and T. Carmon, Flying couplers above spinning resonators generate irreversible refraction, *Nature (London)* **558**, 569 (2018).
- [33] H. Jing, H. Lü, S. K. Özdemir, T. Carmon, and F. Nori, Nanoparticle sensing with a spinning resonator, *Optica* **5**, 1424 (2018).
- [34] B. Li, R. Huang, X.-W. Xu, A. Miranowicz, and H. Jing, Nonreciprocal unconventional photon blockade in a spinning optomechanical system, *Photon. Res.* **7**, 630 (2019).
- [35] K. Wang, Q. Wu, Y.-F. Yu, and Z.-M. Zhang, Nonreciprocal photon blockade in a two-mode cavity with a second-order nonlinearity, *Phys. Rev. A* **100**, 053832 (2019).
- [36] H. Z. Shen, Q. Wang, J. Wang, and X. X. Yi, Nonreciprocal unconventional photon blockade in a driven dissipative cavity with parametric amplification, *Phys. Rev. A* **101**, 013826 (2020).
- [37] W. S. Xue, H. Z. Shen, and X. X. Yi, Nonreciprocal conventional photon blockade in driven dissipative atom-cavity, *Opt. Lett.* **45**, 4424 (2020).
- [38] X.-W. Xu, Y. Zhao, H. Wang, H. Jing, and A. Chen, Quantum nonreciprocity in quadratic optomechanics, *Photon. Res.* **8**, 143 (2020).
- [39] X.-W. Xu, Y. Li, B. Li, H. Jing, and A.-X. Chen, Nonreciprocity via Nonlinearity and Synthetic Magnetism, *Phys. Rev. Appl.* **13**, 044070 (2020).
- [40] P. Yang, M. Li, X. Han, H. He, G. Li, C.-L. Zou, P. Zhang, and T. Zhang, Non-reciprocal cavity polariton, *arXiv:1911.10300*.
- [41] C. W. Gardiner and M. J. Collett, Input and output in damped quantum systems: Quantum stochastic differential equations and the master equation, *Phys. Rev. A* **31**, 3761 (1985).
- [42] H. Carmichael, *An Open Systems Approach to Quantum Optics* (Springer-Verlag, Berlin, 1993).
- [43] Y. Li, Y. Y. Huang, X. Z. Zhang, and L. Tian, Optical directional amplification in a three-mode optomechanical system, *Opt. Express* **25**, 18907 (2017).
- [44] X. Z. Zhang, L. Tian, and Y. Li, Optomechanical transistor with mechanical gain, *Phys. Rev. A* **97**, 043818 (2018).
- [45] C. Jiang, L. N. Song, and Y. Li, Directional amplifier in an optomechanical system with optical gain, *Phys. Rev. A* **97**, 053812 (2018).
- [46] Z. Shen, Y. Zhang, Y. Chen, F.-W. Sun, X.-B. Zou, G.-C. Guo, C.-L. Zou, and C. Dong, Reconfigurable optomechanical circulator and directional amplifier, *Nat. Commun.* **9**, 1797 (2018).
- [47] L. Mercier de Lépinay, E. Damskäg, C. F. Ockeloen-Korppi, and M. A. Sillanpää, Realization of directional amplification in a microwave optomechanical device, *Phys. Rev. Appl.* **11**, 034027 (2019).
- [48] T. Aoki, B. Dayan, E. Wilcut, W. Bowen, A. Parkins, T. Kippenberg, K. Vahala, and H. Kimble, Observation of strong coupling between one atom and a monolithic microresonator, *Nature (London)* **443**, 671 (2006).
- [49] D. W. Vernoooy, V. S. Ilchenko, H. Mabuchi, E. W. Streed, and H. J. Kimble, High- $Q$  measurements of fused-silica microspheres in the near infrared, *Opt. Lett.* **23**, 247 (1998).
- [50] S. M. Spillane, T. J. Kippenberg, K. J. Vahala, K. W. Goh, E. Wilcut, and H. J. Kimble, Ultrahigh- $Q$  toroidal microresonators for cavity quantum electrodynamics, *Phys. Rev. A* **71**, 013817 (2005).
- [51] I. S. Grudinin, V. S. Ilchenko, and L. Maleki, Ultrahigh optical  $Q$  factors of crystalline resonators in the linear regime, *Phys. Rev. A* **74**, 063806 (2006).
- [52] A. A. Savchenkov, A. B. Matsko, V. S. Ilchenko, and L. Maleki, Optical resonators with ten million finesse, *Opt. Express* **15**, 6768 (2007).
- [53] V. Huet, A. Rasoloniaina, P. Guillemé, P. Rochard, P. Féron, M. Mortier, A. Levenson, K. Bencheikh, A. Yacomotti, and Y. Dumeige, Millisecond Photon Lifetime in a Slow-Light Microcavity, *Phys. Rev. Lett.* **116**, 133902 (2016).
- [54] H. Lee, T. Chen, J. Li, K. Y. Yang, S. Jeon, O. Painter, and K. J. Vahala, Chemically etched ultrahigh- $Q$  wedge-resonator on a silicon chip, *Nat. Photonics* **6**, 369 (2012).
- [55] Y.-F. Jiao, S.-D. Zhang, Y.-L. Zhang, A. Miranowicz, L.-M. Kuang, and H. Jing, Nonreciprocal Optomechanical Entanglement against Backscattering Losses, *Phys. Rev. Lett.* **125**, 143605 (2020).
- [56] W. T. M. Irvine, K. Hennessy, and D. Bouwmeester, Strong Coupling between Single Photons in Semiconductor Microcavities, *Phys. Rev. Lett.* **96**, 057405 (2006).
- [57] X. Guo, C.-L. Zou, H. Jung, and H. X. Tang, On-Chip Strong Coupling and Efficient Frequency Conversion between Telecom and Visible Optical Modes, *Phys. Rev. Lett.* **117**, 123902 (2016).
- [58] J.-H. Chen, X. Shen, S.-J. Tang, Q.-T. Cao, Q. Gong, and Y.-F. Xiao, Microcavity Nonlinear Optics with an Organically Functionalized Surface, *Phys. Rev. Lett.* **123**, 173902 (2019).
- [59] Q.-T. Cao, R. Liu, H. Wang, Y.-K. Lu, C.-W. Qiu, S. Rotter, Q. Gong, and Y.-F. Xiao, Reconfigurable symmetry-broken laser in a symmetric microcavity, *Nat. Commun.* **11**, 1136 (2020).

- [60] H. Choi, M. Heuck, and D. Englund, Self-Similar Nanocavity Design with Ultrasmall Mode Volume for Single-Photon Nonlinearities, *Phys. Rev. Lett.* **118**, 223605 (2017).
- [61] M. Aspelmeyer, T. J. Kippenberg, and F. Marquardt, Cavity optomechanics, *Rev. Mod. Phys.* **86**, 1391 (2014).
- [62] Z. H. Wang, C. P. Sun, and Y. Li, Microwave degenerate parametric down-conversion with a single cyclic three-level system in a circuit-qed setup, *Phys. Rev. A* **91**, 043801 (2015).
- [63] M. Gullans, D. E. Chang, F. H. L. Koppens, F. J. Garcia de Abajo, and M. D. Lukin, Single-Photon Nonlinear Optics with Graphene Plasmons, *Phys. Rev. Lett.* **111**, 247401 (2013).
- [64] I. A. Calafell, J. D. Cox, M. Radonjic, J. R. M. Saavedra, F. J. Garcia de Abajo, L. A. Rozema, and P. Walther, Author correction: Quantum computing with graphene plasmons, *npj Quantum Inf.* **5**, 37 (2019).